

Electron–polar optical phonon scattering suppression and mobility enhancement in wurtzite heterostructures

E P Pokatilov^{1,2}, D L Nika^{1,2}, N D Zincenco² and A A Balandin¹

¹Nano-Device Laboratory, Department of Electrical Engineering, University of California – Riverside, Riverside, California 92521 USA

²Department of Theoretical Physics, State University of Moldova, Kishinev, MD 2009 Moldova

E-mail: balandin@ee.ucr.edu

Abstract. We have shown theoretically that the electron mobility in wurtzite AlN/GaN/AlN heterostructures can be enhanced by compensating the built-in electric field with the externally applied perpendicular electric field and by introducing a shallow $\text{In}_x\text{Ga}_{1-x}\text{N}$ channel in the center of GaN potential well. It was found that two- to fivefold increase of the room temperature electron mobility can be achieved. The tuning of the electron mobility with the external electric field or $\text{In}_x\text{Ga}_{1-x}\text{N}$ channel can be useful for the design of GaN-based field-effect transistors and optoelectronic devices.

1. Introduction

The electron mobility in polar semiconductors at room temperature is limited by the electron – phonon scattering [1]. The strength of the electron – phonon interaction in semiconductor nano- and heterostructures depends on the electron wave function and energy spectrum as well as on the optical and acoustic phonon dispersion. By changing geometry and material parameters of heterostructures one can affect both the carrier and phonon spectrum. Controlled modification of the electron spectrum is conventionally referred to as electron band-structure engineering [1] while tuning the phonon modes has been termed as phonon engineering [2].

In this paper we show that the electron mobility can be enhanced in heterostructures made of wurtzite AlGaIn/GaN/AlGaIn semiconductors via (i) adjustment of their built-in electric field, and (ii) via introduction of the narrow InGaIn channel, also referred to as nanogroove, in the center of GaN quantum well with a small Indium (In) content. Depending on the electron concentration, applied field and In content, the mobility can manifest rather unexpected non-monotonic character. This finding and the prospect of the room-temperature mobility enhancement can potentially influence the design of the GaN-based optoelectronic devices or high-power field-effect transistors. Indeed, the reduced scattering may lead to faster devices and better thermal management of GaN transistors [3].

2. Theoretical Model

We consider two types of wurtzite heterostructures: AlN/GaN/AlN (3 nm/ 6 nm/ 3 nm) and AlN/GaN/ $\text{In}_x\text{Ga}_{1-x}\text{N}$ /GaN/AlN (3 nm/ 3 nm/ 2 nm/ 3nm/ 3nm). To account for the inter-subband transitions in QWs we derived the system of two integral equations for the electron kinetic relaxation times. This system is the extension of the Boltzmann transport equation introduced in the convenient

form in Ref. [4]. The system of two integral equations has been modified to include the phonon dispersion. The modified equations, derived under the assumption of a spherical electron Brillouin zone, are written as [5-6]

$$\sum_{\substack{\vec{p}', m=\pm 1, \\ \lambda, n=1, 2}} [W(n, \vec{p} \rightarrow n', \vec{p}') \frac{(1 - f^0(\varepsilon_n + m \cdot \hbar \omega_\lambda(q)))}{(1 - f^0(\varepsilon_n))} (\tau_n(\vec{p}) - \tau_{n'}(\vec{p}') \frac{\vec{p} \cdot \vec{p}'}{p^2})] = 1, \quad (1)$$

where $n=1, 2$. In Equation (1) $W(\gamma \rightarrow \gamma') = 2\pi / \hbar \cdot \left| \langle \gamma' | \hat{H}_{IF}^S + \hat{H}_{IF}^A + \hat{H}_C^S + \hat{H}_C^A | \gamma \rangle \right|^2 \delta(E_\gamma - E_{\gamma'})$ is the probability of a transition of the electron – phonon system from the state γ with energy E_γ to the state γ' with the energy $E_{\gamma'}$, $f^0(\varepsilon) = (\exp(\frac{\varepsilon - \varepsilon_F}{k_B T}) + 1)^{-1}$, ε is the electron energy, q is the phonon wave vector, \vec{p} and \vec{p}' are the electron momentum in the initial and final states, λ is the polarization index (quantum number) of the confined and interface optical phonon branches, $\tau_1(\varepsilon)$ is the kinetic relaxation time of an electron with energy ε in the first (ground) subband, which includes electron transitions within the first subband ($1 \leftrightarrow 1$) and transitions from the first to the second subband ($1 \rightarrow 2$), $\tau_2(\varepsilon)$ is the kinetic relaxation time of an electron in the second subband, which includes transitions from the second to the first subband ($2 \rightarrow 1$) and the transitions within the second subband ($2 \leftrightarrow 2$).

The electron mobility was calculated using the expression

$$\mu(T) = \frac{e}{k_B T} \frac{\sum_{n=1}^2 \frac{1}{m_{\perp, n}} \int_0^\infty \varepsilon \tau_n(\varepsilon) f^0(\varepsilon) (1 - f^0(\varepsilon)) d\varepsilon}{\sum_{n=1}^2 \int_0^\infty f^0(\varepsilon_n^0 + \varepsilon) d\varepsilon}, \quad (2)$$

where e is the electron charge and $m_{\perp, n}$ is the effective electron mass, averaged by electron wave functions of n -th energy level (see for details Ref. [7]). Note that Equation (2) takes into account both the intra-subband and inter-subband transitions. To solve Equation (1) we generated a mesh with the step of 0.2 meV. The upper boundary energy of $\varepsilon_{\max} = 600$ meV was chosen from the condition $\varepsilon_{\max} \gg \hbar \omega_{opt}$. The system of $2N$ ($N=3001$) linear equations for the values of τ_1 and τ_2 in the nodal points ε_l ($l=1, \dots, N$) has been solved numerically. The system of the equations was terminated with the condition $\varepsilon_l + \hbar \omega(q) \approx \varepsilon_N$ when $\varepsilon_l + \hbar \omega(q) > \varepsilon_N$ ($\varepsilon_N = \varepsilon_{\max} \gg \hbar \omega_{opt}$). The calculated relaxation times were plugged into Equation (2) to obtain the mobility.

3. Results and Discussion

The Hamiltonians of interaction of electrons with the symmetric (S) and asymmetric (A) confined (C) and interface (IF) optical phonon modes, i.e., \hat{H}_{IF}^S , \hat{H}_{IF}^A , \hat{H}_C^S and \hat{H}_C^A , in AlN/GaN/AlN heterostructure were taken from Ref. [8]. The material parameters required for mobility calculations in wurtzite AlN/GaN/AlN and AlN/GaN/In_xGa_{1-x}N/GaN/AlN heterostructures were taken from Refs. [8-9]. The intra-subband scattering in the ground state ($1 \leftrightarrow 1$) is determined by the matrix element $M_{11} = \int_{-d/2}^{d/2} \varphi_{n=1}^2 V_{IF,C}^{S,A} dz$, where d is the width of the whole heterostructure, φ_n is the electron wave function (w.f.) of n -th size-quantized level, $V_{IF,C}^{S,A}$ is the potential for the symmetric (S), antisymmetric (A), confined (C) or interface (IF) optical phonon modes. The intensity of the built-in electric field $F_{built-in}$ due to the spontaneous and induced piezoelectric polarization in AlN/GaN/AlN quantum wells (QW) reaches several MV/cm [10]. With increasing resulting electrical field $\mathfrak{F} = F_{built-in} - F_{ext}$ (where F_{ext} is the

external electric field applied perpendicular to heterostructure cladding layers) this matrix element increases mostly due to the w.f. $\varphi_{n=1}(z)$ shift to the QW interface and growth of its maximum. When $\mathcal{F}=0$, the built-in electric field is entirely compensated by the perpendicular external field: $F_{built-in}=F_{ext}$ and only S phonon modes contribute to the matrix element. The intensity of the inter-subband electron transitions ($1\leftrightarrow 2$) is determined by (i) the value of the energy difference $\varepsilon_2^0 - \varepsilon_F$ (ε_2^0 is the energy of the first excited states, while ε_F is the Fermi energy) and (ii) the matrix element $M_{12} = \int_{-d/2}^{d/2} \varphi_{n=1}\varphi_{n=2}V_{IF,C}^{S,A}dz$. When $\varepsilon_2^0 - \varepsilon_F$ becomes larger than the phonon energy $\hbar\omega$ the inter-subband transitions stop. For $\mathcal{F}=0$, w.f. $\varphi_{n=2}$ is antisymmetric and, correspondingly, transitions are generated by antisymmetric phonon modes.

The dependence of the electron mobility on the resulting electric field is shown in Figure 1 (a) for two temperatures $T=250$ K and $T=300$ K. The results are presented for the electron density $N_s=5 \cdot 10^{12}$ cm⁻². With increasing \mathcal{F} the energy gap between subbands widens and the intra-subband scattering becomes the only scattering mechanism. The effect of the uncompensated field $\mathcal{F}\neq 0$ is two-fold. From one side, the field reduces inter-subband scattering ($1\rightarrow 2$), but enhances intra-subband scattering ($1\leftrightarrow 1$). Weakening of the inter-subband transitions leads even to a moderate growth of μ and appearance of a maximum near $\mathcal{F}\sim 700$ kV/cm for both considered temperatures. Note that the electron mobility calculated taking into account the intra-subband scattering only monotonically enhances with decreasing of \mathcal{F} due to decreasing of the matrix element M_{11} (corresponding curves are shown in Figure 1 (a) by dotted lines).

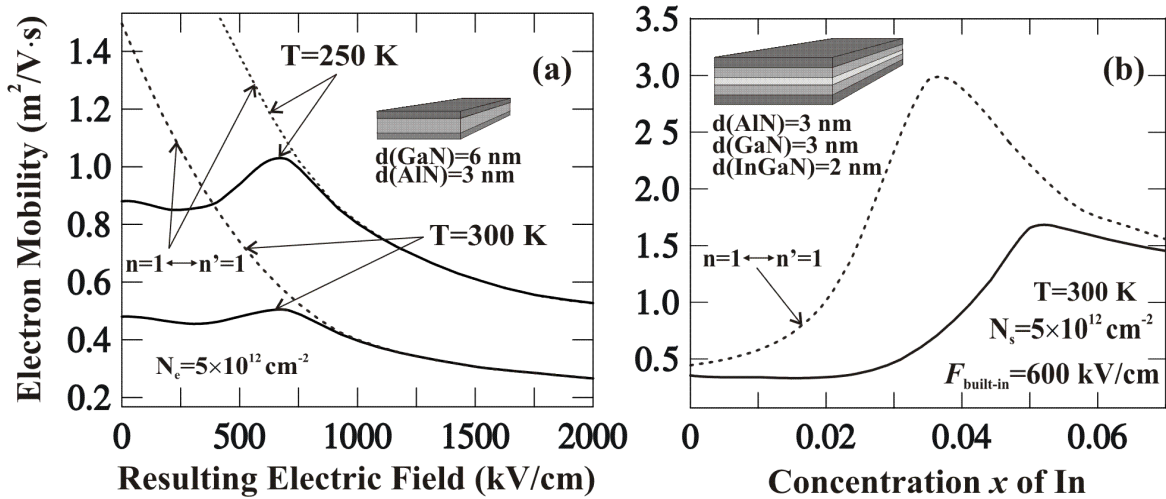


Figure 1. The dependence of electron mobility (a) on the resulting electric field in AlN/GaN/AlN heterostructure and (b) on the Indium content x in AlN/GaN/In _{x} Ga_{1- x} N/GaN/AlN heterostructure.

The room-temperature electron mobility μ in AlN/GaN/In _{x} Ga_{1- x} N/GaN/AlN heterostructure, calculated as a function of x , is shown in Figure 1 (b) for the electron density $N_s=5 \cdot 10^{12}$ cm⁻². The initial mobility reduction in the interval $0 < x \leq 0.02$ is explained by the enhanced inter-subband scattering due to the proximity of ε_2^0 and E_F energy levels. Further increase of In content in the In _{x} Ga_{1- x} N nanogroove ($x \geq 0.04$) leads to a gradual suppression of the inter-subband transitions (via

stronger wave function localization), and weakening of the electron interaction with the AlN/GaN interface phonon modes owing to the w.f. shift to the QW center. At the same time, the electron interaction with the confined optical phonons starts to grow due to the increase of the electron density in the middle of QW. The interplay of these trends results in achieving a maximum mobility for x in the range 0.045–0.055. For $x \geq 0.055$, the mechanisms, which led to the mobility enhancement (weakening of the inter-subband transitions and suppression of the electron – interface optical phonon scattering) become less effective while increased localization of the electron w.f. results in growing strength of the electron interaction with confined optical phonons. The latter explains the mobility reduction for $x > 0.055$. In Figure 1 (b) we also show the electron mobility (dotted curve), which was calculated assuming the intra-subband ($1 \leftarrow \rightarrow 1$) scattering only, and by completely neglecting $1 \leftarrow \rightarrow 2$ and $2 \leftarrow \rightarrow 2$ scattering transitions. As one can see, this curve strongly differs from the mobility calculated with all relevant scattering mechanisms (solid curve). This confirms that in the considered heterostructures the inter-subband electron transitions play an important role. The results presented in Figure 1 indicate that room temperature electron mobility is enhanced by a factor of ~ 2 for AlN/GaN/AlN heterostructure with the compensated electric field (with the initial built-in field between 2000–4000 KV/cm) and by a factor of ~ 5 for AlN/GaN/In_{0.05}Ga_{0.95}N/GaN/AlN heterostructure in comparison with generic heterostructure without In_{0.05}Ga_{0.95}N nanogroove.

4. Conclusions

We have shown that the electron mobility in wurtzite GaN-based heterostructures with strong built-in electric field can be enhanced by compensating the built-in field with the external perpendicular electric field or by introduction of the narrow In_xGa_{1-x}N nanogroove in the middle of the GaN potential well with a small Indium content (2–5 %). The non-monotonic dependence of the mobility on the electric field and Indium content is explained by the interplay of the intra- and intersubband scattering processes. The predicted effects can be used for engineering the electronic properties of wurtzite GaN-based nanostructures.

Acknowledgements

The work was supported in part by US Civil Research and Development Foundation (CRDF) through the grant MOE2-3057-CS-03 and the State Projects of Republic of Moldova no. 06.408.036F and 06.35.CRF. The work at UCR was also supported, in part, by the MARCO Center on Functional Engineered Nano Architectonics (FENA).

References

- [1] Singh J 1993 *Physics of Semiconductors and Their Heterostructures* (McGraw-Hill, New York)
- [2] Balandin A A and Wang K L 1998 *Phys. Rev. B* **58** 1544; Pokatilov E P, Nika D L and Balandin A A 2005 *Phys. Rev. B* **72** 113311
- [3] Liu W L, Turin V O, Balandin A A, Chen Y L and Wang K L 2004 *MRS J. of Nitride Semiconductor Research* **9** 7; Turin V O and Balandin A A 2006 *J. Appl. Phys.* **100** 054501
- [4] Bannov N, Aristov V, Mitin V and Strosio M A 1995 *Phys. Rev. B* **51** 9930
- [5] Pokatilov E P, Nika D L and Balandin A A 2006 *Appl. Phys. Lett.* **89** 112110; 2006 *Appl. Phys. Lett.* **89** 113508
- [6] Balandin A A, Pokatilov E P and Nika D L 2007 *J. Nanoelectron. Optoelectron.* **2** 140
- [7] Pokatilov E P, Nika D L and Balandin A A 2004 *J. Appl. Phys.* **95** 5626
- [8] Lee B C, Kim K W, Strosio M A and Dutta M 1998 *Phys. Rev. B* **58** 4860
- [9] Vurgaftman I and Meyer J R 2003 *J. Appl. Phys.* **94** 3675
- [10] Adelman C, Sarigiannidou E, Jalabert D, Hori Y, Rouviere J L, Daudin B, Fanget S, Bru-Chevalier C, Shibata T and Tanaka M 2003 *Appl. Phys. Lett.* **82** 4154